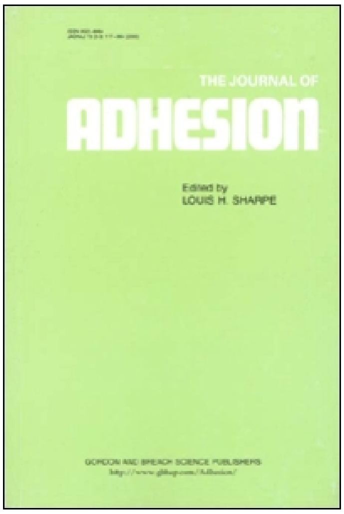

The Journal of Adhesion
Publication details, including instructions for authors and subscription information:
http://www.informaworld.com/smpp/title~content=t713453635

Crack growth in adhesively bonded joints subjected to variable frequency fatigue loading

A. H. Al-Ghamdi[a]; I. A. Ashcroft[a]; A. D. Crocombe[b]; M. M. Abdel-Wahab[b]
[a] Wolfson School of Mechanical and Manufacturing Engineering, Loughborough University, Leicestershire, UK [b] School of Mechanical and Materials Engineering, University of Surrey, Guildford, UK

Online publication date: 08 September 2010

To cite this Article Al-Ghamdi, A. H. , Ashcroft, I. A. , Crocombe, A. D. and Abdel-Wahab, M. M.(2003) 'Crack growth in adhesively bonded joints subjected to variable frequency fatigue loading', The Journal of Adhesion, 79: 12, 1161 — 1182
To link to this Article: DOI: 10.1080/714906165
URL: http://dx.doi.org/10.1080/714906165

The Journal of Adhesion, 79: 1161–1182, 2003

ISSN: 0021-8464 print/1545-5823 online
DOI: 10.1080/00218460390268254

CRACK GROWTH IN ADHESIVELY BONDED JOINTS SUBJECTED TO VARIABLE FREQUENCY FATIGUE LOADING

A. H. Al-Ghamdi
I. A. Ashcroft
Wolfson School of Mechanical and Manufacturing Engineering, Loughborough University, Leicestershire, UK

A. D. Crocombe
M. M. Abdel-Wahab
School of Mechanical and Materials Engineering, University of Surrey, Guildford, UK

The main aim of this article is to investigate the effect of frequency on fatigue crack propagation in adhesively bonded joints. Adhesively bonded double-cantilever beam (DCB) samples were tested in fatigue at various frequencies between 0.1 and 10 Hz. The adhesive used was a toughened epoxy, and the substrates used were a carbon fibre-reinforced polymer (CFRP) and mild steel. Results showed that the crack growth per cycle increases and the fatigue threshold decreases as the test frequency decreases. The locus of failure with the CFRP adherends was predominantly in the adhesive layer, whereas the locus of failure with the steel adherends was in the interfacial region between the steel and the adhesive. The crack growth was faster, for a given strain energy release rate, and the fatigue thresholds lower for the samples with steel adherends. Tests with variable frequency loading were also carried out, and a generalised method of predicting crack growth in samples subjected to a variable frequency loading was introduced. The predicted crack growth using this method agreed well with experimental results.

Keywords: Fatigue; Frequency; Epoxy adhesive; CFRP; Mild steel; DCB

Received 28 May 2003; in final form 2 October 2003.
Address correspondence to I. A. Ashcroft, Wolfson School of Mechanical and Manufacturing Engineering, Loughborough University, Loughborough, Leicestershire, LE11 3TU, UK. E-mail: i.a.ashcroft@lboro.ac.uk

INTRODUCTION

The increasing use of adhesives has created a need to evaluate their performance under many different loading and environmental conditions. Many adhesive joints are subject to cyclic loads during service, such as bonded bridge-strengthening plates and aircraft fuselages [1]. Since adhesive joints are less tolerant of cyclic than of static loading, there has been considerable research work into various aspects of the fatigue behaviour of adhesive joints [2–12]. The time span of each fatigue load cycle can vary significantly from one structure to another. It could be, for instance, several seconds in the case of bridge plates to tens of hours in the case of aircraft fuselages and in many applications variable fatigue frequencies are encountered in service. The time taken to generate fatigue data means that most fatigue testing of bonded joints has been undertaken at relatively high frequencies, typically 5–10 Hz. However, the visco-elastic nature of polymeric adhesives means that rate and frequency dependence might be expected and that this would increase at elevated temperatures or when the adhesive has absorbed moisture. There is, therefore, a requirement to understand the effect of frequency on the fatigue life of bonded joints and how parameters such as joint geometry, environment, and materials affect this behaviour. Ideally, a general method of predicting fatigue life at any given frequency (or combination of frequencies and hold times) should be developed. This is the aim of the current work.

The effect of frequency on fatigue crack propagation (FCP) in metals has been extensively investigated. For instance, James [13–14] demonstrated the influence of frequency and waveform on fatigue crack growth in a stainless steel. This work showed that the fatigue crack propagation rate (FCPR) increased with decreasing frequency. It should be noted here that FCPR is defined as the crack growth per fatigue cycle, *i.e.*, da/dN, where a is crack growth and N is number of cycles. A similar study demonstrated that the FCPR increased with hold time in a trapezoidal loading waveform for a Cr-Mo-V steel [15]. Plumtree and Yu [16] also showed that for a 304 stainless steel the time-dependent damage accumulates more rapidly during the loading portion of the cycle than during the hold time. Prenotched samples of a number of polymers have also been tested in fatigue over a range of frequencies [17–20]. The FCPR for several of these polymers, such as polymethyl methacrylate, polystyrene, polyvinyl chloride, and a polyphenylene oxide, decreased with increasing frequency. Other polymers such as polycarbonate, polysulfone, nylon, and a polyvinylidene fluoride showed no apparent sensitivity to test frequency [17–20].

The effect of frequency on the performance of adhesively bonded joints has also been considered previously. Marceau *et al.* [21] studied fatigue crack growth rates in both lap-shear and double cantilever beam (DCB) joints at a range of frequencies and found that low frequency fatigue was more damaging to adhesive joints than high frequency fatigue. Althof [22] studied the buildup of shear strain in adhesive joints during fatigue loading at a range of frequencies and suggested that fatigue failure is creep-controlled at low frequencies. Mostovoy and Ripling [23] used bonded tapered double cantilever beam (TDCB) specimens to study the effect of frequency on the FCPR in different adhesive systems. For a standard amine-cured epoxy, there was no discernible effect of frequency between 0.01 and 0.25 Hz; however, at 3 Hz the FCPR decreased significantly. A standard nitrile-phenolic film adhesive exhibited no significant effect of frequency in the range 0.01–3 Hz. With a modified epoxy adhesive, no effect of frequency was observed on increasing the frequency from 0.25–3 Hz; however, at 5 Hz the FCPR decreased. Luckyram and Vardy [24] studied the fatigue performance of two structural adhesive and found no effect of frequency on FCPR between 0.5–5 Hz. Likewise, Osiyemi [25] found no effect of frequency on the FCPR in composite DCB joints bonded with a 120°C cure epoxy film adhesive in the frequency range 1–5 Hz. Xu *et al.* [26] studied the effect of frequency on FCP using steel DCB joints bonded with two structural epoxy adhesives. Adhesive A was filled with a mixture of magnesium silicate and chalk and tested at frequencies of 2 and 20 Hz. Adhesive B was rubber-toughened and was tested at frequencies of 0.02, 0.2, 2, and 20 Hz. They found that the FCPR for adhesive A was relatively independent of frequency, whilst the FCPR in joints bonded with adhesive B decreased with increasing frequency. Pirondi and Nicoletto [27] studied the effect of R-ratio and frequency on fatigue crack growth in bonded steel DCBs. The threshold value of ΔG seemed to be insensitive to frequency between 5 and 10 Hz, but the shape of the FCP curves varied, which was attributed to the strong viscoelastic nature of the adhesive used. It can be seen from the above that the sensitivity of FCPR in adhesives is material-dependent but that there is a tendency in many systems for the FCPR to increase as frequency decreases. This is a concern, as most fatigue data are generated at relatively high frequencies, which will tend to lead to nonconservative predictions of fatigue life if applied to joints subjected to lower frequencies.

In this work, the effect of frequency on FCPR and the fatigue threshold for adhesively bonded DCB joints with carbon fibre-reinforced polymer (CFRP) and mild steel substrates are compared.

The selection of different substrates and pretreatments enables FCPR for different failure loci to be compared. The majority of the fatigue characterization of bonded joints in laboratories is under constant frequency. The applied frequency in many real structures fluctuates randomly, creating a frequency spectrum, or the frequency could vary in sequential steps, resulting in a block frequency loading. In this work, FCPR for joints subjected to a variable block frequency loading is investigated and a generalised numerical procedure for predicting the variable frequency fatigue life of adhesively bonded structures is proposed.

EXPERIMENTAL DETAILS

Experimental Materials

The CFRP used in this study was IM7/8552, supplied by Hexcel Composites (Duxford, UK), which consists of intermediate modulus graphite fibres in an epoxy matrix (IM7/8552). The other adherend material used was mild steel. The mechanical properties of unidirectional panels of the CFRP and the mild steel are given in Table 1. The adhesive used was Cytec's FM300-2M (Cytec, West Patterson, NJ, USA). This is a single-part toughened epoxy film that has a random mat carrier and nominal thickness of 0.2 mm. The Young's modulus and Poisson's ratio of the adhesive are 2.45 GPa and 0.38, respectively [28].

CFRP Joint Manufacture

Unidirectional CFRP pre-preg was laid up with uncured adhesive film, FM300-2M, to manufacture the CFRP DCB samples. A thin film (nominally 10 μm) of poly(tetrafluoroethylene) (PTFE) was placed at the bond line at one end of the panels to act as a starter crack. This assembly was autoclave cured at 180°C for 2 h with a pressure of 0.6 MPa, as dictated by the advised curing schedule for the CFRP pre-preg. This process, in which both adhesive and CFRP are cured in the same treatment, is termed cobonding and can be compared with

TABLE 1 Material Properties

Material	E_x (GPa)	E_y (GPa)	G_{xy} (GPA)	v_{xy}	v_{yx}
IM7-8552	164.41	11.72	5.516	0.36	0.02
Mild steel	209	—	—	0.3	0.3

secondary bonding, in which the CFRP is cured before being bonded, and cocuring, in which composite parts are joined without an adhesive layer. The adhesive chosen for this study is a dual cure adhesive that is recommended for cobonding CFRP and also for secondary bonding metals and can be cured in the temperature range 120–180°C. After curing the cobonded panels, a diamond saw was used to cut the samples to the dimensions shown in Figure 1. Brass hinges were bonded to the joint with a high peel strength adhesive that was cured overnight at 55°C. The width of the test specimen was 25 mm and other dimensions as shown in Figure 1.

Mild Steel Joint Manufacture

The mild steel substrates were grit blasted and degreased prior to bonding. The cleaned and dried substrates were then coated with BR-127 primer, which was applied to the substrates by brush and air dried for 30 min prior to an oven cure for 30 min at 120°C. As with the CFRP samples, a thin film of PTFE was placed at the bond line at one end of the panels to act as a starter crack. This assembly was cured for 2 h at 120°C with a pressure of 0.28 MPa. Note that without the need to cure the CFRP pre-preg, the adhesive could be cured at a lower temperature than in the case of the cobonded CFRP samples. It is possible that the different curing temperature may affect the mechanical properties of the adhesive or the state of residual stress

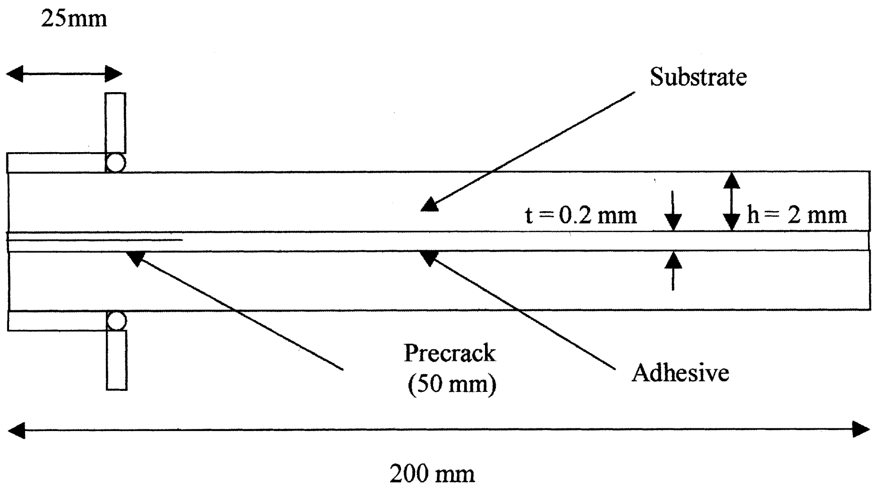

FIGURE 1 Double cantilever beam specimen with CFRP substrates.

in the joints. In this instance these effects need not be explicitly analysed; however, it should be remembered that they might have an affect on the FCP curves. After curing, an electrical saw and milling machine were used to cut the samples to the dimensions shown in Figure 2. The width of the test specimen was 25 mm, and the other dimensions were as shown in Figure 2.

Fatigue Testing

The experimental arrangement is shown in Figure 3. Testing was carried out using a servo hydraulic test machine fitted with computer control and data acquisition. The crack length variation during the fatigue testing was measured using the commercial "Krak-Gage" and "Fractomat" system supplied by RUMUL. The "Krak-Gage" is a thin (~5 μm) constantan metalfoil, which is adhesively bonded to the side of a test specimen. During fracture of the sample, the "Krak-Gage" is designed to tear coincidentally with the crack in the actual test specimen. The change in resistance as the Krak-Gage tears is measured by the Fractomat and converted to a crack length. The output from the Fractomat was input to the computer data acquisition system *via* a strain channel on the test machine. Direct observations of crack length were made using a travelling microscope as a second check on the measured crack length.

Testing was carried out under displacement control with constant amplitude sinusoidal waveforms, displacement ratios (*i.e.*, min. disp./max. disp.) of $R = 0.1$ and a range of frequencies (10 Hz, 5 Hz, 1 Hz, and 0.1 Hz). The variable frequency-loading regime consisted of

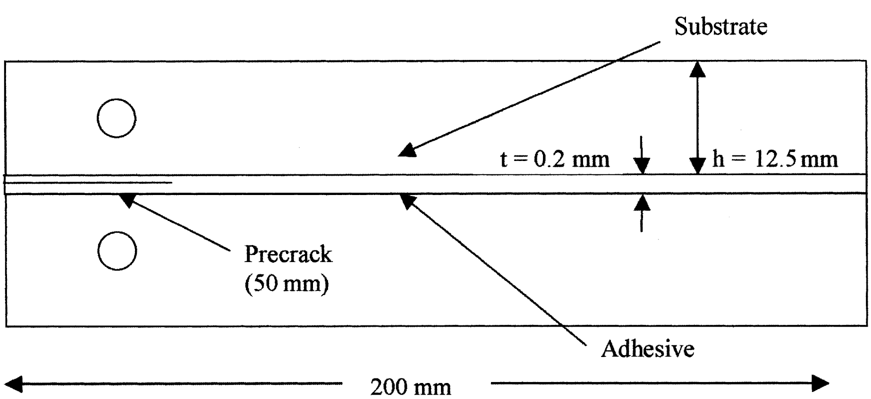

FIGURE 2 Double cantilever beam specimen with steel substrates.

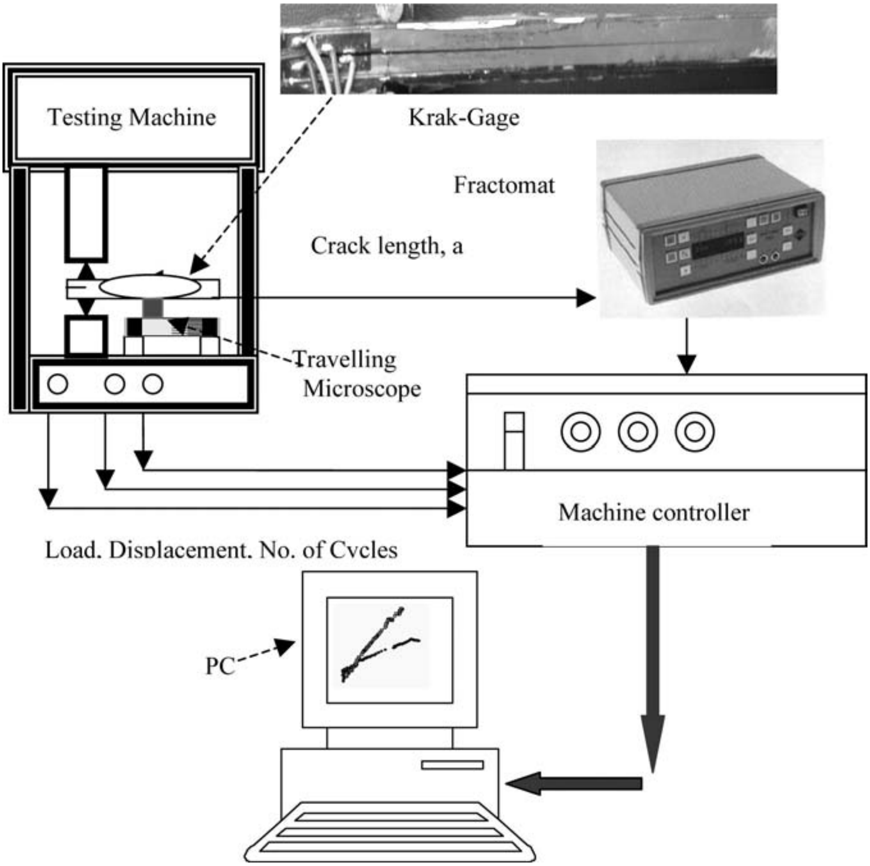

FIGURE 3 Fatigue test configuration.

a three-stage block loading spectrum with frequencies of 10 Hz, 1 Hz, and 0.1 Hz. The number of cycles in each stage was 1000. Two to three samples were tested for each case, and mean values were calculated.

Fractography

The fracture surfaces were examined using both optical and scanning electron microscopy (SEM). Optical microscopy was used to study the locus of failure and to examine the appearance of the fracture surface. Samples for SEM analysis were then extracted and mounted on metal stubs. The CFRP samples were coated to ensure electrical conductivity.

DATA ANALYSIS

Experimentally, the principal measurements are crack length, load, and displacement as a function of cycles. The next step in the characterisation of FCP in the sample is to calculate the strain energy release rate and the FCPR as a function of cycles from these experimental data. Methods of performing these calculations are described below.

Calculation of Strain Energy Release Rate (G)

The value of G at peak load ($G_{\max}$) was determined using a beam on elastic foundation model. This method was originally developed by Kanninen [29]. Each half of the beam is considered as a beam partly free and partly supported by an elastic foundation. This model has been simplified [30] to give the following equation for strain energy release rate:

$$G_I = \frac{12P^2}{b^2h^3E}(a+\Delta)^2, \tag{1}$$

$$\Delta^4 = \frac{4EIt}{E_a b}, \tag{2}$$

where P is the load; a is the crack length; E_a is the Young's modulus of the adhesive; t is the thickness of the foundation (*i.e.*, half the thickness of the adhesive); Δ serves as a length scale; h and b are the thickness and width of the beam, respectively; and EI is its flexural rigidity. This equation is based on the assumptions that shear energy is negligible and that d/Δ is comparable to or greater than 2π, where d is the uncracked length of the beam.

Calculation of the Fatigue Crack Propagation Rate (FCPR)

The FCPR is defined as da/dN, where a is the crack length and N is the number of fatigue cycles. In this work, the seven-point incremental polynomial method was used to calculate the FCPR. This method is recommended in the standard test method ASTM E647-86a and involves fitting a second-order polynomial to a group of seven successive data points. The rates are then obtained by differentiating the fitted equation. The characteristic equations for this procedure are given below:

$$a = b_0 + b_1\left[\frac{N-C_1}{C_2}\right] + b_2\left[\frac{N-C_1}{C_2}\right]^2, \tag{3}$$

where b_0, b_1 and b_2 are regression parameters that are determined by applying the method of least squares to the data set. The terms C_1 and C_2 are used to scale the input data in order to avoid numerical difficulties in this process. The fatigue crack growth rate is then obtained by differentiating Equation (3) with respect to N:

$$\frac{da}{dN} = \frac{b_1}{C_2} + 2b_2\left[\frac{N - C_1}{C_2^2}\right], \tag{4}$$

An Excel macro was written using Visual Basic for Applications (VBA) to aid analysis using the approaches described above.

Variable Frequency Fatigue Prediction Procedure

In previous work by a number of authors [31–36] attempts have been made to predict the fatigue performance of adhesively bonded joints. In this article an attempt is made to extend this work to the prediction of fatigue crack growth under variable frequency loading. This is based on first obtaining constant amplitude fatigue crack propagation (FCP) curves (*i.e.*, plotting da/dN *vs.* $G_{\max}$) within the desired frequency range. The crack growth rate, da/dN, can be correlated to a suitable fracture mechanics parameter using a suitable fatigue law, such as the Paris law [37]:

$$\frac{da}{dN} = D(G_{\max})^n. \tag{5}$$

To perform the predictions, the values for the Paris law coefficients, D and n, need to be derived from the experimental data. These coefficients along with the threshold strain energy release rate (G_{th}) and the critical strain energy release rate (G_{c}) are all that are required to describe the FCP curve and can be considered as material properties. This has been done for both type of joints at 10 Hz, 1 Hz, and 0.1 Hz and the results are summarised in Table 2. The fatigue law constants at intermediate frequencies could be obtained by interpolation from the known experimental value, and the method is equally applicable to cases where other fracture parameters or fatigue laws are more appropriate. EXCEL solver was used to fit the Paris Law to the experimental data in this case.

Prediction of crack length in variable frequency fatigue is based on a simple iterative algorithm in which $G_{\max}$ is first calculated for the initial crack length, a_0. The Paris law constants for that particular frequency are then used to determine the crack growth rate, da/dN, which is multiplied by the number of cycles in the stage to give the

TABLE 2 Summary of Fatigue Results

Joint type	Frequency (Hz)	G_{th} (J/m^2)	Failure type	Paris constant n	Paris constant D
CFRP FM300-2M	10	220	Cohesive	3.35	2.59E-16
CFRP FM300-2M	1	187	Cohesive	3.25	1.00E-15
CFRP FM300-2M	0.1	140	Cohesive	2.99	1.58E-14
Mild steel FM300-2M	10	133	Interfacial	3.12	2.11E-15
Mild steel FM300-2M	1	111	Interfacial	2.95	2.71E-14
Mild steel FM300-2M	0.1	82	Interfacial	2.59	4.52E-13

overall crack growth during the stage (Δa). A new crack size ($a_1 = a_0 + \Delta a$) is then calculated and the process repeated. This procedure is repeated until G_{max} becomes equal to the threshold value, G_{th}, in displacement control or until G_{max} equals G_c in load control. It can be seen that this is a simple method that is valid if there are no significant interaction or load history effects. The size of each iterative stage was reduced until negligible change in predicted behaviour was seen. The steps used in this prediction method are illustrated in Figure 4.

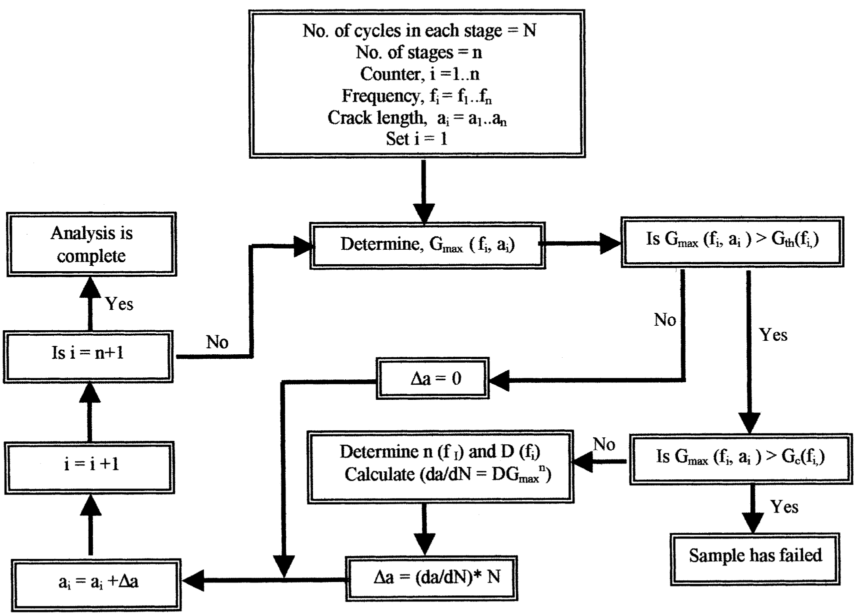

FIGURE 4 Fatigue life prediction algorithm.

RESULTS

The locus of failure from optical and SEM examination of the fracture surfaces was found to be predominantly cohesive failure of the adhesive for the CFRP joints. In the case of the steel DCBs, failure was predominantly in the interfacial region between the adhesive and adherend with occasional small islands of cohesive fracture. For both types of adherend there was no discernible change in the appearance of the fracture surface as frequency changed. Two to three samples were tested for each load case, and the calculated mean values used to construct the FCP curves. Repeatability of the tests was generally good as illustrated in Figure 5, which shows the FCP curves for three CFRP specimens tested at 10 Hz.

Constant Frequency Fatigue Tests

Log-log plots of FCPR against G_{max} for the CFRP and mild steel DCBs are shown in Figures 6 and 7 respectively. Both figures clearly show

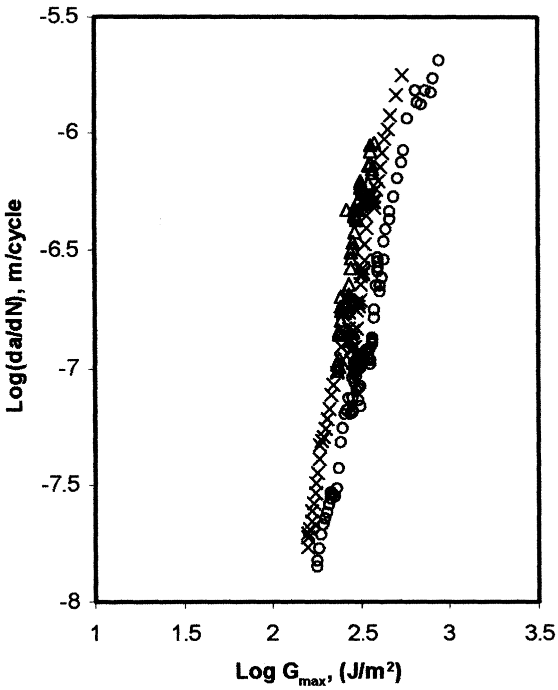

FIGURE 5 FCP curves of three CFRP samples tested at 10 Hz.

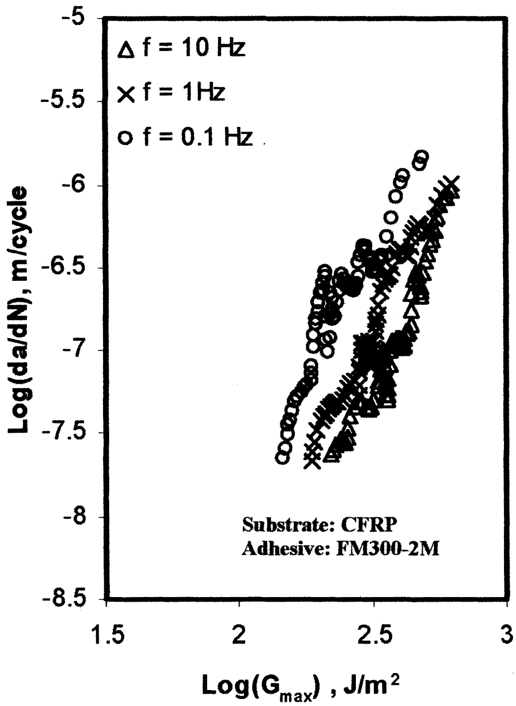

FIGURE 6 FCP curves for CFRP joints in terms of da/dN.

the effect of fatigue frequency. The fatigue threshold (G_{th}), *i.e.*, the value of G_{max} below which fatigue crack growth is negligible, can be seen to decrease as the test frequency decreases. At $G_{max} > G_{th}$, it can be seen that the crack growth is faster at low frequencies for both types of joints. Comparison of Figures 6 and 7 also shows that the FCPR is much faster in the mild steel joints than in the CFRP joints. The frequency sensitivity factor (FSF), defined as the multiple by which the FCPR changes per decade change in test frequency, is approximately 1.1 for the CFRP DCBs and 1.2 for the mild steel joints. Fatigue crack growth rates were reprocessed in terms of da/dt, and the log-log plot of da/dt *versus* G_{max} is plotted in Figures 8 and 9 for the CFRP and mild steel, respectively. It is seen that the treatment indeed brought the fatigue crack growth rates much closer to each other for the mild steel joints but that there is still a significant difference between curves for the CFRP joints. It can also be seen that when plotting crack growth as a function of time, the crack growth rate for a given value of G_{max} is greater at higher frequencies, which is in

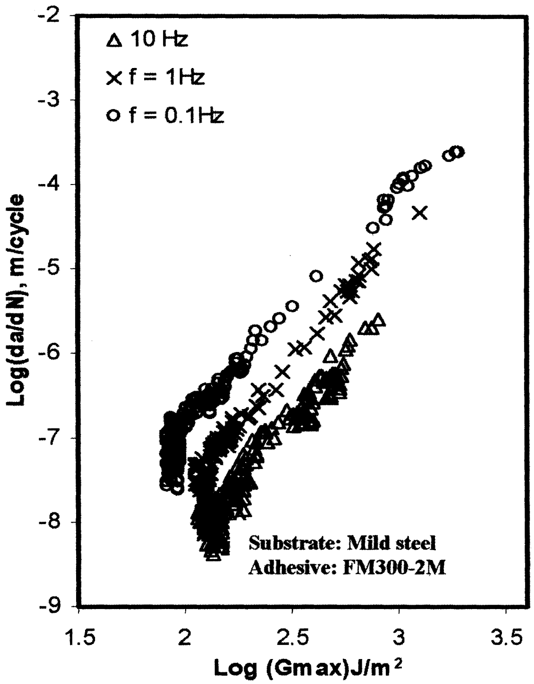

FIGURE 7 FCP curves for mild steel joints in terms of da/dN.

contrast to the trend seen when crack growth is plotted as a function of cycles (*i.e.*, FCGR). It can be said, therefore, that for both substrates fatigue crack growth is dependent on both time and number of cycles, but that in the case of interfacial failure crack growth is time dominated. This means that, as a first approximation, fatigue crack growth for interfacial failure at any frequency can be estimated from a single curve fit through the data points in Figure 8. Table 2 summarises the results of the fatigue tests for the CFRP and mild steel DCB samples.

Variable Frequency Fatigue Tests

Variable frequency testing was carried out using a three-stage block-loading spectrum. The applied frequency for stages 1, 2, and 3 were 10 Hz, 1 Hz, and 0.1 Hz, respectively. The number of cycles in each stage was 1000. Figures 10 and 11 show the experimental crack growth under variable frequency loading and that predicted using the procedure outlined in Figure 4 for CFRP and mild steel joints, respectively. It is clear that there is good agreement between the

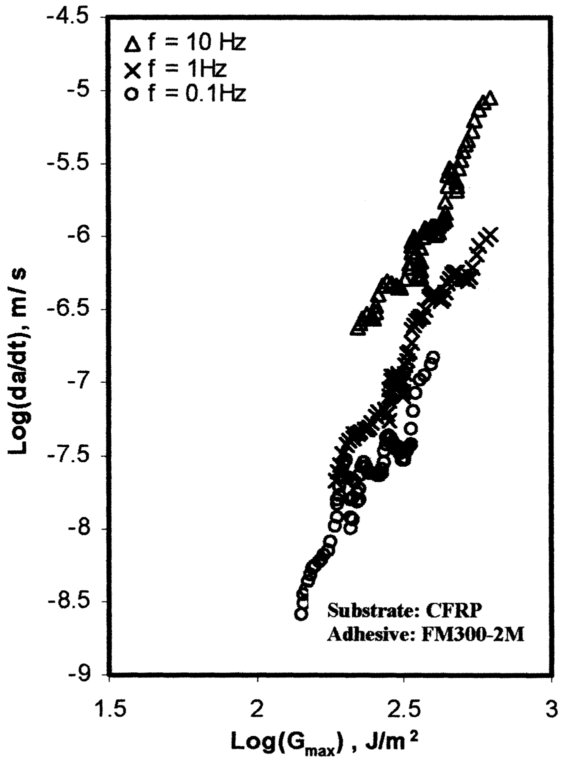

FIGURE 8 FCP curves for CFRP joints in terms of da/dt.

experimental tests and the prediction method. The degree of accuracy of this method depends on the values of the Paris constants, D and n, from the constant frequency tests and the assumption of no interaction or load history effects. The former can be checked by using the prediction algorithm to predict crack growth in the constant frequency tests. This is demonstrated in Figure 12, which shows the correlation between the experimental and predicted data crack growth for the 1 Hz constant frequency test. The good agreement indicates that the method of computing the Paris law coefficients and the crack growth prediction algorithm itself are reliable and that any differences between the predicted and experimental crack growth are real. The slight tendency to underestimate variable frequency crack growth may, therefore, indicate a small acceleration effect in the variable frequency spectrum. However, this could also be experimental scatter. In

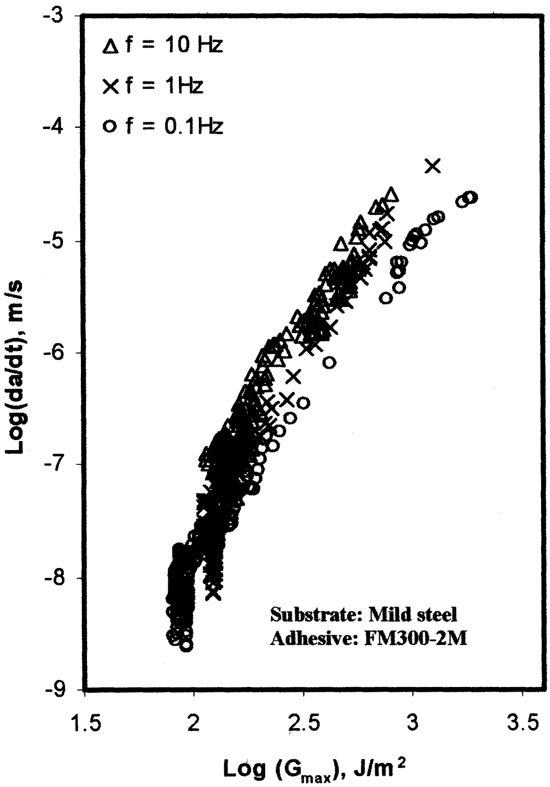

FIGURE 9 FCP curves for mild steel joints in terms of da/dt.

either case it is considered that any such effects are of insufficient importance to warrant inclusion in the predictive algorithm.

DISCUSSION

In this investigation efforts have been made to study the effect of applied frequency on crack growth in bonded DCB samples with mild steel and CFRP substrates. It is seen that for both cohesive and interfacial failure, reducing the fatigue frequency has a significant effect in reducing the fatigue threshold and accelerating crack growth for adhesively bonded joints. By reducing the fatigue frequency from 10 to 0.1 Hz, the threshold value of G_{max} decreases by 64% and 61% for DCBs with CFRP and mild steel substrates, respectively. This effect is most probably attributable to the viscoelastic nature of the

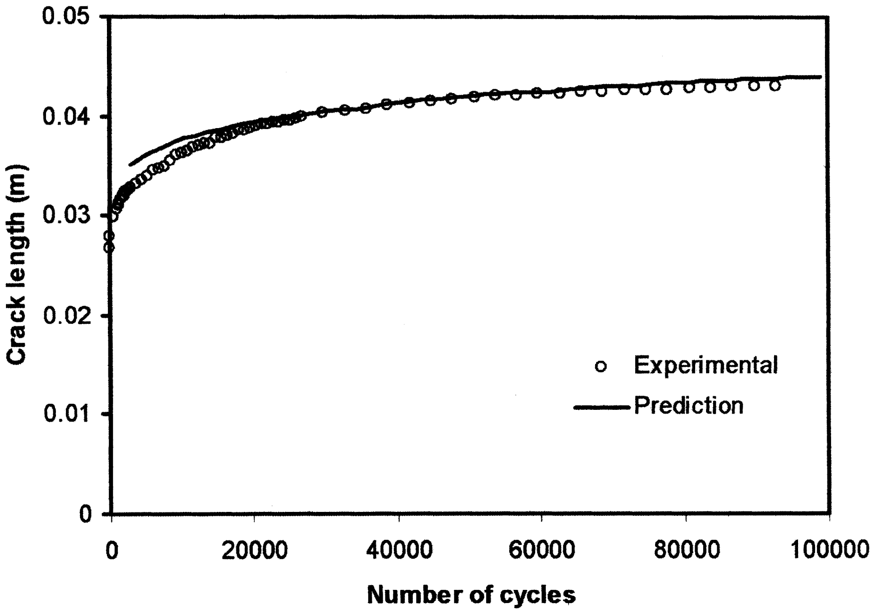

FIGURE 10 Crack growth under variable amplitude loading for CFRP joints.

polymeric materials used in adhesives, which make them rate-sensitive and susceptible to creep. As the loading in this case is always in tension, there may be a significant creep contribution to crack growth, which will increase as the frequency decreases, as the time under load per cycle will increase. This argument is in agreement with many studies [7,8] that have shown that modern adhesives may exhibit significant creep behaviour within their prescribed service range. This result indicates that designers should not use high frequency test data to predict the time to failure of bonded joints subjected to low frequency loading. There is a temptation to do this as the shorter time required to complete a series of high frequency tests means that these data are more commonly available. However, whilst this may be an acceptable practice for some materials, it is inadvisable with polymeric materials, as this will result in nonconservative predictions. It should also be noted that this effect would be expected to worsen as temperature increases or as moisture is absorbed by the adhesive. This is further explored by plotting the crack growth rate as a function of time rather than number of cycles, *i.e.*, da/dt. In the case of interfacial failure this brought the crack growth curves at different frequencies much closer together. This demonstrates that crack growth is more dependent on

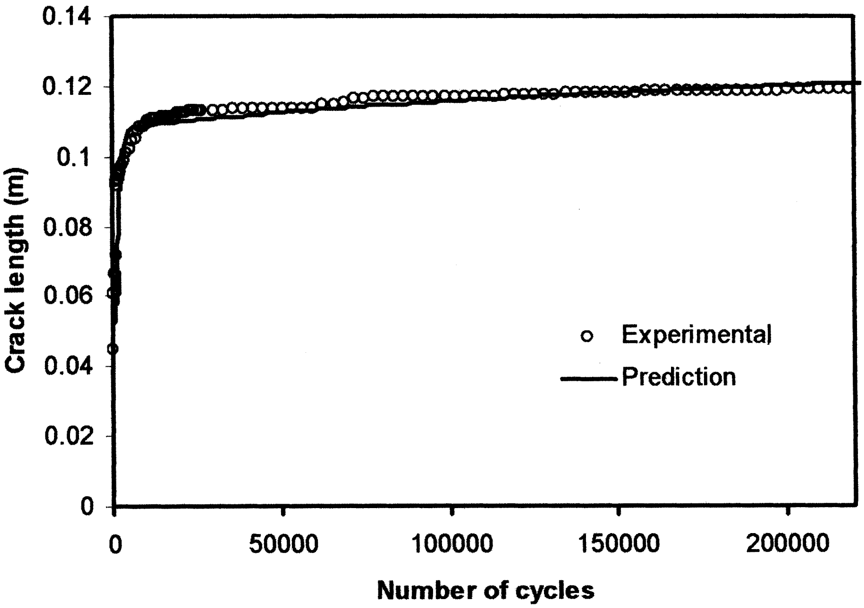

FIGURE 11 Crack growth under variable amplitude loading for mild steel joints.

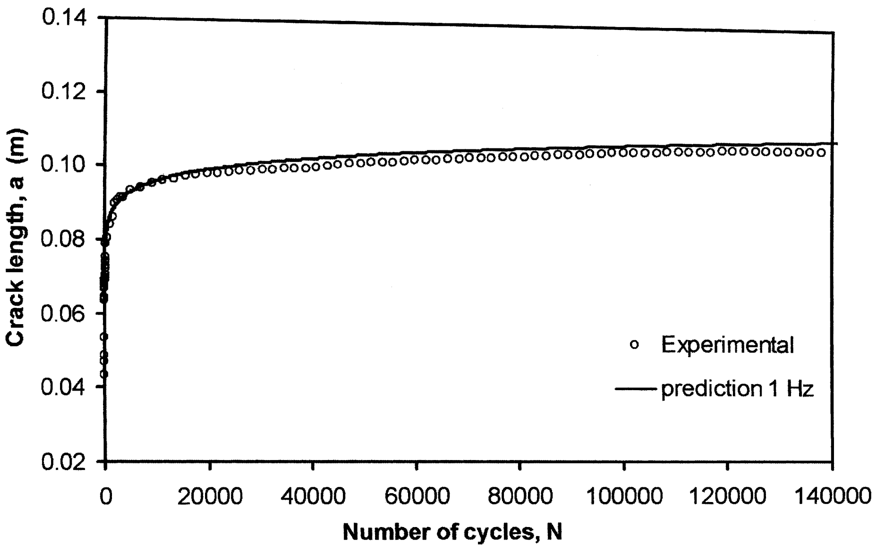

FIGURE 12 Experimental and predicted crack growth at 1 Hz.

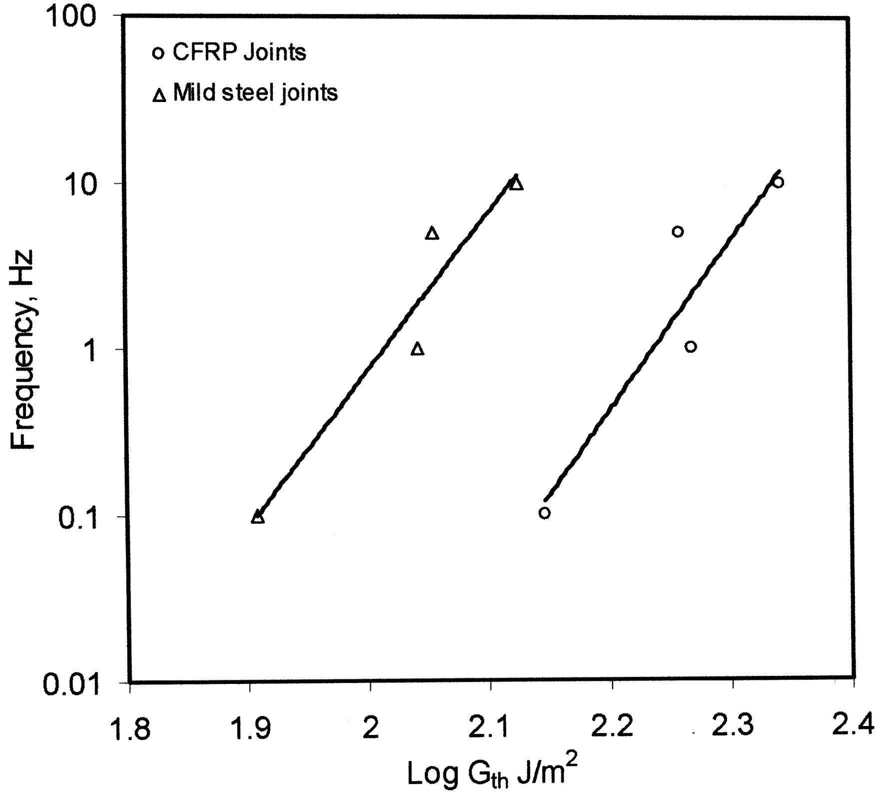

FIGURE 13 The effect of frequency on fatigue threshold.

time under load than number of cycles and as a first approximation crack growth at any frequency can be estimated from a master da/dt *versus* $G_{\max}$ plot.

The threshold strain energy release rate is a potentially useful design criterion, as this can be used to determine the load below which fatigue crack growth is negligible. It is clear from Figure 13 that the fatigue threshold values for the CFRP joints are significantly higher (approximately 60%) than those seen with the mild steel joints at all frequencies. This is not surprising, as the DCBs with mild steel substrates failed interfacially whilst those with the CFRP substrates failed cohesively in the adhesive. It can also be seen that there is a linear relationship between log frequency and log G_{th} for both cohesive and interfacial crack growth, meaning that prediction of fatigue thresholds at other frequencies should be reasonably reliable. It is remarkable how close the slope of the plots of fatigue threshold against frequency are for the two different failure modes; even deviations from the trend line appear to be identical for the two sets of results. This indicates that the fatigue resistance is influenced by the nature of the adhesive in both cases. The results in Table 2 show, as indicated by the Paris law exponents n and D, that crack growth is faster with the mild steel substrates than with the CFRP substrates.

The proposed technique for predicting fatigue life under variable fatigue loading showed good agreement with the experimental results for both cohesive and interfacial failure. This technique could easily be implemented within a design code for predicting fatigue under variable frequency conditions. It would also be a simple matter to include a routine for predicting the Paris law coefficients for frequencies between those determined experimentally using some form of interpolation. Figure 14 and 15 show the relationship between frequency and Paris constant n and D, respectively, for both joints. It can be seen that n increases slightly with frequency for both types of joint whilst D

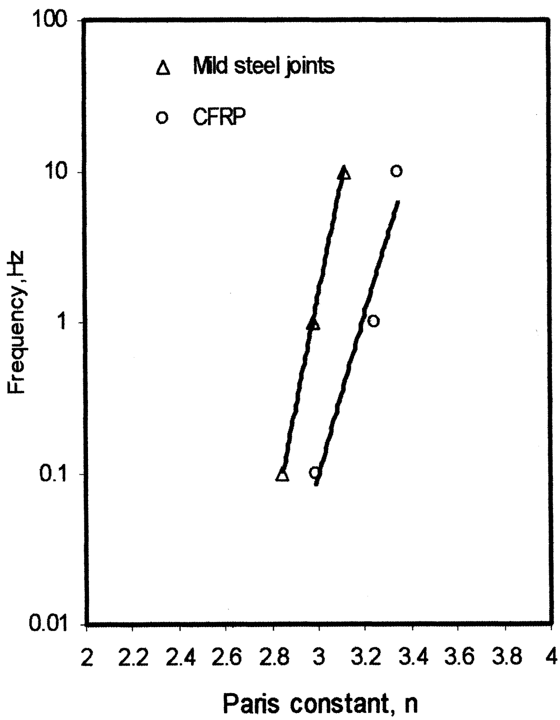

FIGURE 14 The effect of frequency on the Paris constant, n.

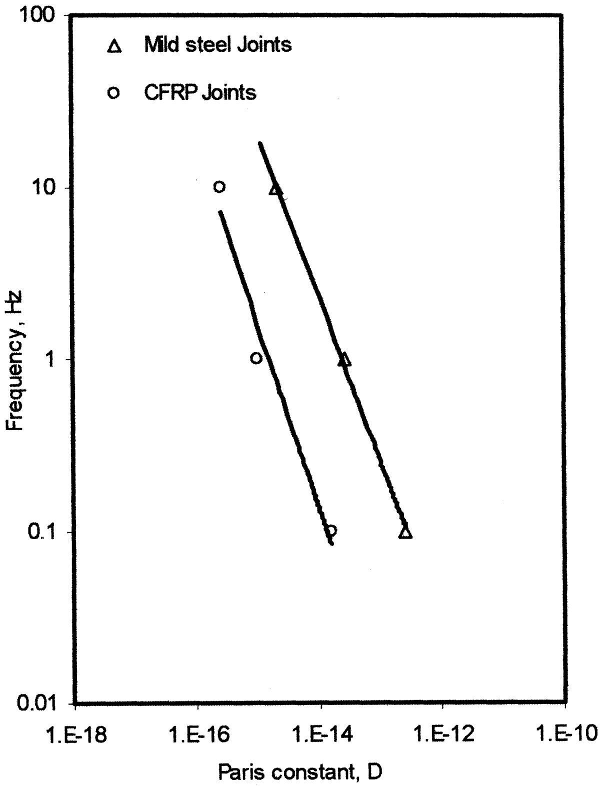

FIGURE 15 The effect of frequency on the Paris constant, D.

decreases as frequency increases. These trends are explained by looking at Figures 6 and 7, where it can be seen that as frequency decreases the slope of the FCP curves vary little but the whole curve is shifted to the left, explaining the decrease in G_{th} and the increase in D. It can be seen from Figures 13–15 that linear relationships have now been obtained between log frequency and log G_{th}, D and n. This is significant as it means that a FCP curve can be easily constructed for any frequency and, hence, crack growth at any frequency, or variable frequency spectrum can be easily predicted using the algorithm in Figure 4.

CONCLUSIONS

The effects of constant and variable frequency fatigue loading on mode I crack growth for mild steel and CFRP DCBs bonded with an epoxy adhesive have been investigated. The following conclusions were obtained.

1. The fatigue threshold decreases and the fatigue crack propagation rate increases as the fatigue frequency is reduced from 10 to 0.1 Hz. Fatigue threshold can be used by designers to predict the fatigue load a bonded structure can withstand without crack growth.
2. Linear relationships were seen between log frequency and log G_{th}, D and n. These relationships can be used to construct a FCP curve and, hence, predict crack growth at any frequency.
3. The fatigue threshold values for the CFRP joints (cohesive failure) are higher than those for the mild steel joints (interfacial failure) for all frequencies. Crack growth between G_{th} and G_c is greater in the mild steel joints for a given value of G_{max}.
4. The prediction of variable frequency fatigue using a simple damage accumulation method based on the Paris Law agreed well with the experimental results. This is potentially useful for designers to estimate the fatigue life of bonded joints subjected to complex loading spectra. The procedure has the following steps:

   a. Determine the parameters D, n, G_c, and G_{th} over the required frequency range and use interpolation to calculate the value of these parameters at intermediate frequencies.
   b. Determine G_{max} (or some other fracture mechanics parameter) as a function of crack length for the structure to be analysed and use the method shown in Figure 4 to predict crack growth as a function of number of cycles or time.

REFERENCES

[1] Adams, R. D., Comyn, J. and Wake, W. C., *Structural Adhesive Joints in Engineering* (Chapman and Hall Publishers, London, 1997), pp. 7–9.
[2] Mall, S., *Fatigue Behaviour of Adhesively Bonded Joints* NASA-CR-174458 (1983).
[3] Mall, S., Ramamurthy, G. and Rezaizdeh, M. A., *Composite Structures* **8**, 31–37 (1987).
[4] Ashcroft, I. A., Gilmore, R. B. and Shaw, S. J., AGARD CP-590, NATO,14.1–14.9 (1996).
[5] Dessureault, M. and Spelt, J. K., *Int. J. Adhesion Adhesives* **17**, 183–185 (1997).
[6] Ashcroft, I. A., Hughes, D. J. and Shaw, S. J., *Assembly Automation* **20**, 150–156 (2000).
[7] Xu, X. X., Crocombe, A. D. and Smith, P. A., *J. Adhesion* **58**, 191–194 (1995).
[8] Ashcroft, I. A., Hughes, D. J., Shaw, S. J., Abdel-Wahab, M. M. and Crocombe, A. D., *J. Adhesion* **75**, 61–88 (2001).
[9] Ashcroft, I. A., Abdel-Wahab, M. M., Crocombe, A. D., Hughes, D. J. and Shaw, S. J., *Composites Part A* **32**, 45–50 (2001).
[10] Crocombe, A. D., Ong, A. D., Chan, C. Y., Abdel-Wahab, M. M. and Ashcroft, I. A., *J. Adhesion* **78**, 745–752 (2002).

[11] Erpolat, S., Ashcroft, I. A., Crocombe, A. D. and Abdel-Wahab, M. M., *Proc. 26th Annual Meeting of the Adhesion Society*, Anderson, G. L., Ed. The Adhesion Society, Blacksburg, VA, USA (2003), pp. 74–76.
[12] Al-Ghamdi, A. H., Ashcroft, I. A., Crocombe, A. D. and Abdel-Wahab, M. M., *Proc. Euradh 2002/Adhesion 02, Institute of Materials Communications, London, (2002), pp. 190–193.*
[13] James, L. A., ASTM STP 513, (American Society for Testing and Materials, Philadelphia, PA, 1972), pp. 218–229.
[14] James, L. A., *Nuclear Technology* **16**, 521–526 (1972).
[15] Saxena, A. and Bassani, J. L., *Interactions of Microstructure, Mechanisms and Mechanics*, TMS-AIME, (1984), pp. 357–383.
[16] Plumtree, A. and Yu, M., *Thermal and Environmental Effects in Fatigue*: *Research-Design Interface*, C. Jaske, S. Hudak and M. Mayfield, Eds. (*American Society for Mechanical Engineers, New York, 1983*), pp. 13–19.
[17] Thorkildsen, R. L., *Engineering Design for Plastics*, E. Baer, Ed. (Van Nostrand-Reinhold, New York 1964), pp. 279–283.
[18] Bucknall, C. B., Gotham, K. V., and Vincent, P. I., *Polymer Science Handbook*, Vol. 1, Chapter 10, (Elsevier, London, 1972).
[19] Skibo, M. D., Manson, J. A., Hertzberg, R. W. and Collins, E. A., *Durability of Macromolecular Materials*, ACS Symposium Series No.95; (American Chemical Society, weighing ton, DC, 1979), pp. 311–315.
[20] Hertzberg, R. W. and Manson, J. A., *Fatigue of Engineering Plastics* (Academic Press, New York 1980), pp. 83–96.
[21] Marceau, J. A., McMillan, J. C. and Scardino, W. M., *Proc. 2nd SAMPE Symposium and Exhibition*, (1977), pp. 64–80.
[22] Althof, W., *Proc. Int. Symp on Adhesive Joints: Formation, Characteristics and Testing*, K. L. Mittal, Ed. (Plenum Press, New York 1984), pp. 659–677.
[23] Mostovoy, S. and Ripling, E. J., *Polym. Sci. Technology* 9B 513–562 (1975).
[24] Luckyram, J. and Vardy, A. E., *J. Adhesion* **26**, 273–291 (1988).
[25] Osiyemi, S. O., The Fatigue Performance of Adhesively Bonded Fibre-Composite Joints Ph.D thesis, Imperial College, London (1992).
[26] Xu, X. X., Crocombe, A. D. and Smith, P. A., *EURADH 94*, SFDV, 232–236, (1994).
[27] Pirondi, A. and Nicoletto, G., *Eng. Fract. Mech.*, in press (2003).
[28] Cheng, Y., Wing, Y. and Sun, J., *Int. J. of Mechanical Sciences* **43**, 2091–2098 (2001).
[29] Kanninen, M. F., *Int. J. Fracture* **9**, 83–92 (1973).
[30] Erpolat, S., Ashcroft, I. A., Crocombe, A. D. and Abdel-Wahab, M. M., *Eng. Fract. Mech.* in press (2003).
[31] Ripling, E. J. and Mostovoy, S., *Application of Fracture Mechanics* ASTM STP360, (American Society for Testing Materials, Philadelphia, PA, USA, 1964).
[32] Abdel-Wahab, M. M., Ashcroft, I. A., Crocombe, A. D., Hughes, D. J., and Shaw, S. J., *Composites Part A* **32**, 59–64 (2001).
[33] Abdel-Wahab, M. M., Ashcroft, I. A., Crocombe, A. D., Hughes, D. J., and Shaw, S. J., *J. Adhesion Sci. Tech.* **15**, 763–772 (2001).
[34] Curley, A., Havadavinia, H., Kinloch, A. J. and Taylor, A. C., *Int. J. Fracture* **103**, 41–49 (2000).
[35] Ashcroft, I. A., and Shaw, S. J., *Int. J. Adhesion Adhesives* **22**, 151–161 (2002).
[36] Abdel Wahab, M. M., Ashcroft, I. A., Crocombe, A. D., and Smith, P. A., *Int. J. Fatigue* **24**, 705–714 (2001).
[37] Paris, P. C., Gomez, M. P. and Anderson, W. E., *Trend Eng.* **13**, 9–14 (1961).